ChemComm

Highly Concentrated Electrolyte Solutions for 4 V Class Potassium-Ion Batteries

Journal:	*ChemComm*
Manuscript ID	CC-COM-06-2018-004433.R1
Article Type:	Communication

Journal Name

COMMUNICATION

Highly Concentrated Electrolyte Solutions for 4 V Class Potassium-Ion Batteries

Received 00th January 20xx,
Accepted 00th January 20xx

DOI: 10.1039/x0xx00000x

www.rsc.org/

Tomooki Hosaka,[a] Kei Kubota,[a,b] Haruka Kojima [a] and Shinichi Komaba *[a,b]

Stable cycling of a 4 V-class potassium-ion battery is demonstrated with a highly concentrated potassium bis(fluorosulfonyl)amide 1,2-dimethoxyethane solution as an electrolyte. Not only graphite and $K_2Mn[Fe(CN)_6]$ half cells but graphite//$K_2Mn[Fe(CN)_6]$ full cells filled with the electrolyte exhibit higher coulombic efficiency and better cyclability than those of KPF_6/carbonate ester solutions.

Lithium-ion batteries (LIBs) have the highest energy density among commercial secondary batteries and are widely utilized for mobile electronic devices, electric vehicles, and energy storage systems. With increasing demand for the large-scale applications, the feasibility of LIBs in the future should be reconsidered because costly and less-abundant lithium, cobalt, and copper are required in 4 V class LIBs, of which average voltage is 3.7 – 3.9 V. In the recent 10 years, sodium-ion batteries (SIBs) and magnesium batteries have been extensively studied as low-cost and material-abundant alternatives to LIBs [1, 2]. More recently, potassium-ion battery (KIB) has attracted much attention because of the possible high-voltage/power operation thanks to a lower standard electrode potential of K/K^+ in organic electrolyte [3] and faster diffusion of K^+ ion in the electrolyte due to its weaker Lewis acidity compared to Li^+, Na^+, and Mg^{2+} ions [4, 5]. To realize KIBs, many researchers have actively developed positive and negative electrode materials for KIBs, but studies on the electrolyte are limited so far.

Electrolytes applicable to KIBs are typically composed of KPF_6, $KClO_4$, KBF_4 or $KN(SO_2F)_2$ (potassium bis(fluorosulfonyl)amide, KFSA) salts dissolved in carbonate ester solvents [5-8]. According to our knowledge, KBF_4 and $KClO_4$ salts are hardly soluble in the carbonate ester solvents unlike the case of $LiBF_4$ and $LiClO_4$ due to high lattice energy of the K salts and low solvation energy of K^+ ion [6, 7]. Since KPF_6 is moderately soluble in carbonate esters and PF_6^- anion is known to passivate Al current collector in LIBs [8], KPF_6 based electrolytes are mainly utilized for KIBs. However, most of the previous studies have suffered from large irreversible capacity especially at the initial cycle and in high voltage operation above 4.0 V, which might originate from the weak oxidation resistant property of the electrolyte and insufficient passivation on the surface of the negative electrode [9-11]. Indeed, graphite negative electrodes in K cell with KPF_6 carbonate ester solution showed low coulombic efficiency in initial cycles, indicating insufficient SEI formation [12]. Development of good electrolytes for KIBs is, therefore, desired to solve these issues such as electrolyte decomposition and passivation, to demonstrate high-energy KIBs.

In Li and Na batteries, highly concentrated electrolytes have attracted interests because of the high oxidation resistant property due to the negligible amount of solvent molecules having no direct coulombic interaction with ions which has a low oxidation stability [13, 14]. In addition, Al corrosion is suppressed in the highly concentrated solution of $LiN(SO_2CF_3)_2$ (LiTFSA) though a 1 mol dm^{-3} LiTFSA/ethylene carbonate (EC):diethyl carbonate (DEC) solution results in the Al corrosion above 3.8 V [15]. Besides, some highly concentrated electrolytes promote the formation of suitable solid electrolyte interphase (SEI) on negative electrode materials such as graphite in LIBs [16], non-graphitizable carbon (so-called hard carbon) in SIBs [17], and Li [18] and Na metals [19, 20]. More recently, a highly concentrated KFSA/1,2-dimethoxyethane (DME) electrolyte solution demonstrated reversible plating of K metal [21]. No systematic researches on the highly concentrated electrolyte were, however, found to demonstrate K^+ ion insertion electrodes for the application of high-voltage KIBs. In this study, we evaluate the ionic conductivities, viscosities, and potential windows of K-based highly concentrated electrolytes and the impact of highly concentrated electrolyte on the electrode performances of $K_2Mn[Fe(CN)_6]$ positive and graphite negative electrode materials in K half-cells and the KIB full cells.

[a] Department of Applied Chemistry, Tokyo University of Science, Shinjuku, Tokyo 162-8601, Japan. E-mail: komaba@rs.kagu.tus.ac.jp
[b] Elements Strategy Initiative for Catalysts and Batteries (ESICB), Kyoto University, 1-30 Goryo-Ohara, Nishikyo-ku, Kyoto 615-8245, Japan
† Electronic supplementary information (ESI) available.

$KN(SO_2CF_3)_2$ (KTFSA, Kanto Chemical), KFSA (Solvionic), $LiN(SO_2F)_2$ (LiFSA, Kanto Chemical), and $NaN(SO_2F)_2$ (NaFSA, Nippon Shokubai) were used as electrolyte salts without any treatment. KPF_6 (Tokyo Chemical Industry) was used after drying at 200 °C for 12 h under vacuum. Battery grade reagents of DME, propylene carbonate (PC), EC, DEC, and γ-butyrolactone (GBL) solvents (Kishida Chemical) were used as received. These salts and solvents were mixed at various molality and stirred for 24 h in an Ar-filled glove box where dew point is < –80 °C. Ionic conductivity measurements of the electrolyte solutions were performed with an ionic conductivity meter (Eutech CON2700, Eutech Instruments) in the glove box at room temperature (28 °C ± 3 °C). The viscosity of the electrolyte solutions was measured with an electromagnetically spinning viscometer (EMS-1000, Kyoto Electronics Manufacturing) at 25 °C. Galvanostatic charge/discharge test and cyclic voltammetry were conducted in a 2032 coin-type cell in which metallic potassium (Sigma-Aldrich) counter electrode and glass fiber separator (GB-100R, Advantec) were used. An Al-clad cathode cap (Hohsen) was used for the coin-type cell to avoid the effect of stainless steel corrosion. An Al working electrode after cyclic voltammetry was observed by 3D laser scanning microscope (VK-X200, Keyence). The working electrodes consisted of 70 wt% $K_2Mn[Fe(CN)_6]$, 20 wt% Ketjen black (KB, Carbon ECP, Lion), and 10 wt% poly(vinylidene fluoride) (PVdF, Kishida Chemical) as positive electrodes and 90 wt% graphite (SNO3, SEC Carbon) and 10 wt% sodium polyacrylate (PANa, Kishida Chemical) binder as negative electrodes of KIB. Both positive and negative electrodes were prepared by coating the slurry on Al foil and dried at 150 °C under vacuum. For full cell tests, 10 wt% PANa was used as a binder of the positive electrode. Mass loading of $K_2Mn[Fe(CN)_6]$ in the electrodes was ca. 0.7 and 1.3 mg cm^{-2} for half-cell and full-cell tests, respectively. $K_2Mn[Fe(CN)_6]$ was synthesized by a precipitation method, and the detailed synthesis condition, composition, and structural parameters refined by Rietveld method were described in the Supporting information, Figures S1 and S2 and Table S1.

Prior to preparation of highly concentrated electrolyte solutions, the solubility of potassium salts in organic solvents was examined at room temperature. Powders of 0.5 mol KFSA, KTFSA, KPF_6, $KClO_4$, and KBF_4 were mixed with PC to obtain 1 dm^3 of their mixtures at room temperature, corresponding molarity and molality of 0.50 mol dm^{-3} and approximately 0.43 mol kg^{-1}, respectively, if the powders are completely dissolved. Figures 1 (a) and (b) show a photograph and ionic conductivity of these mixtures, respectively. White powder visually remained for the case of $KClO_4$ and KBF_4, indicating $KClO_4$ and KBF_4 are hardly dissolved in PC solvent at room temperature. On the other hand, the mixtures of KFSA, KTFSA, and KPF_6 are transparent and colorless liquid without any precipitation, indicating that molar solubility of KFSA, KTFSA, and KPF_6 salts in PC is higher than 0.5 mol dm^{-3}. As expected from the solubility, the KFSA, KTFSA, and KPF_6 solutions show much higher ionic conductivity, ranging between 8 and 5.5 mS cm^{-1}, than those of $KClO_4$ and KBF_4 in Fig. 1 (b). Highly concentrated solutions were, therefore, prepared with KPF_6, KFSA, and KTFSA salts. KPF_6/PC, KPF_6/DME, KTFSA/DME, KFSA/PC, KFSA/DME, and KFSA/GBL solutions were prepared, and their ionic conductivities are compared in Figure 1 (c). KPF_6 was moderately soluble in PC and DME up to 0.9 mol kg^{-1} and 1.8 mol kg^{-1}, respectively, by mixing at room temperature. On the other hand, KFSA is highly soluble in PC up to ca. 10 mol kg^{-1} corresponding to 50/50 mol% in KFSA/PC, and KFSA and KTFSA are also soluble in DME up to ca. 7.5 and 6 mol kg^{-1}, respectively. In addition, KFSA is quite soluble in GBL up to 12 mol kg^{-1} corresponding to 50/50 mol% in KFSA/GBL at room temperature. Not only KFSA shows higher solubility in DME than those of KTFSA and KPF_6 but the KFSA/DME solutions show higher ionic conductivity than KTFSA/DME and KPF_6/DME solutions in Fig. 1(c), which is possibly due to a weak interaction between the FSA^- and K^+ originating from low Lewis basicity of FSA^- [22]. In the KFSA solutions, comparison of the ionic conductivity among PC, DME, and GBL solutions reveals that the ionic conductivity is maximized at 1.5 – 2.0 mol kg^{-1} and the value of the KFSA/DME solution is the highest at a concentration of approximately 2 mol kg^{-1}.

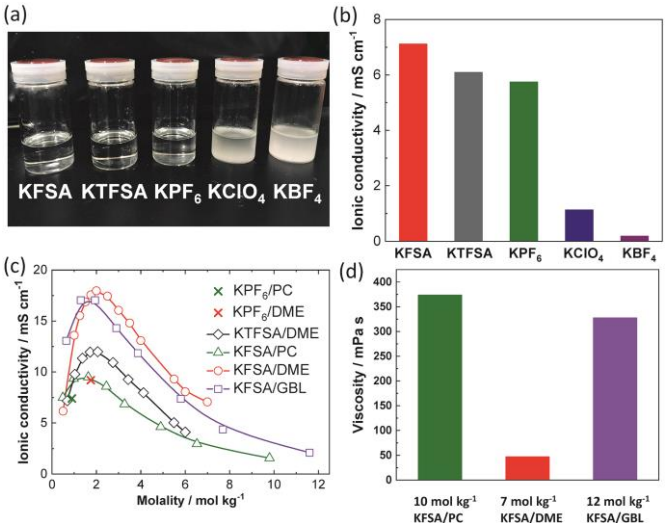

Fig. 1 (a) Photograph of mixtures of KFSA, KTFSA, KPF_6, KBF_4, and $KClO_4$ in PC containing 0.5 mol of salts in 1 dm^3 of mixtures after stirring for 12 h and (b) ionic conductivity of the prepared solutions at 25 °C ±1 °C. (c) Molality vs. ionic conductivity plots of KFSA in DME, GBL, and DME and KTFSA/DME solutions measured at 28 °C ±2 °C and (d) viscosity of 7 mol kg^{-1} KFSA/DME, 12 mol kg^{-1} KFSA/GBL and 10 mol kg^{-1} KFSA/PC at 25 °C

Detailed physical and electrochemical properties of highly concentrated electrolytes, 10 mol kg^{-1} KFSA/PC, 7 mol kg^{-1} KFSA/DME, corresponding to 40/60 mol% in KFSA/DME, and 12 mol kg^{-1} KFSA/GBL solutions were further examined. The viscosity of these solutions is summarized in Fig. 1 (d). The solution of 7 mol kg^{-1} KFSA/DME shows much lower viscosity of 47 mPa s than 374 and 327 mPa s of 10 mol kg^{-1} KFSA/PC and 12 mol kg^{-1} KFSA/GBL, respectively. The lower viscosity will be advantageous for electrolyte penetration into separators and electrodes. Here, ionic conductivity and viscosity of AFSA/DME where A = Li, Na, and K are compared in Fig. S3. Due to the lower Lewis acidity of K^+, KFSA shows the highest ionic conductivity and the lowest viscosity above 2.0 mol kg^{-1} in DME. Indeed, KFSA shows the higher ionic conductivity and the lowest viscosity in PC in 0.5 – 2.0 mol dm^{-3} as we reported [7]. However,

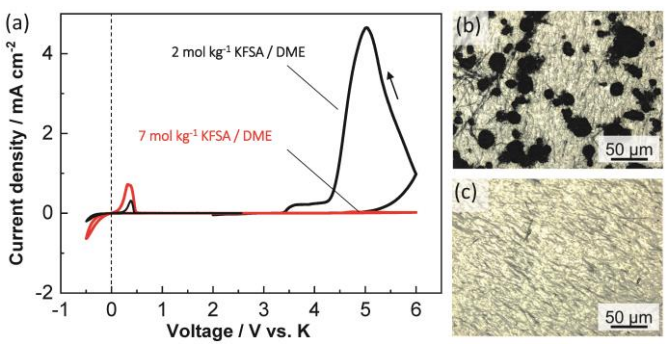

Fig. 2 Potential windows of the electrolytes: (a) cyclic voltammograms of Al working electrodes in 2 mol kg^{-1} and 7 mol kg^{-1} of KFSA/DME solutions at a scanning speed of 0.5 mV s^{-1} in voltage ranges of 2 – -0.5 V and 2 – 6 V in K//Al cell. Microscopic images of Al working electrodes tested in (b) 2 mol kg^{-1} KFSA/DME and (c) 7 mol kg^{-1} KFSA/DME after 3 cycles of CV measurement in voltage ranges of 2 – 6 V.

KFSA solutions showed slightly lower ionic conductivity in the non-concentrated range below 1.5 mol kg^{-1} than LiFSA and NaFSA solutions, which is different from the order of Lewis acidity and would originate from their coordination structures of AFSA/DME probably different from those in PC. The solution structures are under investigation by spectroscopic and computational methods and will be reported elsewhere.

To assess potential window of the highly concentrated KFSA/DME solutions, we conducted cyclic voltammetry (CV) by using two-electrode type K//Al cells. Figure 2 (a) shows initial CV curves of the cells filled with 2 and 7 mol kg^{-1} KFSA/DME electrolytes. Between 2.0 and –0.5 V, both cells show reversible redox around 0 V corresponding to potassium plating. Higher redox current and efficiency of 80.0 % of K plating are achieved in the concentrated solution, indicating better passivation of K surface in the concentrated one. Significant irreversible anodic current above 3.5 V flows only in 2 mol kg^{-1} KFSA/DME. Figure 2 (b) confirms that many pits of 10 – 30 μm in diameter are observed on the Al electrode after 3 cycles in the 2 mol kg^{-1} KFSA/DME cell, which is indicative of Al corrosion [8]. On the other hand, the morphology of Al electrode cycled in 7 mol kg^{-1} KFSA/DME does not change at all in Fig. 2 (c). Therefore, Al corrosion and electrolyte decomposition do not occur in 7 mol kg^{-1} KFSA/DME electrolyte as no apparent anodic/cathodic currents are observed in the voltammogram except for reversible K plating. Thus, wide potential window was demonstrated with inexpensive Al foil in 7 mol kg^{-1} KFSA/DME, which is similar to the previous reports on Li- [15] and Na-based [20] highly concentrated electrolytes. We confirmed that anodic currents are hardly observed in 10 mol kg^{-1} KFSA/PC and 12 mol kg^{-1} KFSA/GBL but some corrosion pits of 1 – 5 μm in diameter are observed on the Al surface after the cycle tests in 2.0 – 6.0 V (see Fig. S4). We believe that the suppression of Al corrosion in the 7 mol kg^{-1} KFSA/DME electrolyte originates from the low dielectric constant of DME as reported in Li-based concentrated electrolytes [23,24]. In addition, negligible anodic current less than 25 μA cm^{-2} is confirmed below 4.3 V in the CV tests for KB and 10 wt% PVdF composite electrodes formed on an Al foil in 7 mol kg^{-1} KFSA/DME (Fig. S5).

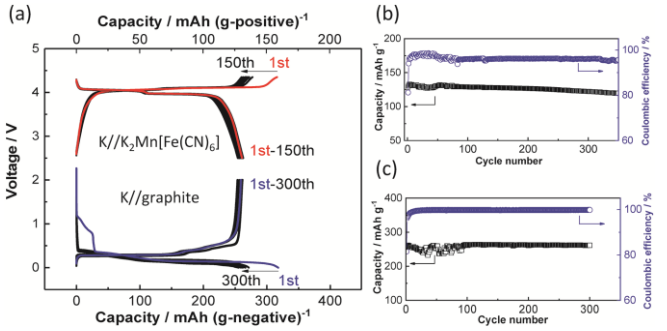

Fig. 3 Electrode performance of the $K_2Mn[Fe(CN)_6]$ and the graphite in K cells: (a) charge/discharge curves of the $K_2Mn[Fe(CN)_6]$ and graphite electrode, and cycle performance and coulombic efficiency of (b) the $K_2Mn[Fe(CN)_6]$ electrode and (c) the graphite electrode.

We assembled and tested the K half-cells of $K_2Mn[Fe(CN)_6]$ and graphite electrodes filled with the highly concentrated KFSA/DME electrolyte. Figure 3 (a) shows that the K//$K_2Mn[Fe(CN)_6]$ cell exhibits initial reversible capacity of 132 mAh g^{-1} in a voltage range of 2.5 – 4.3 V. The initial coulombic efficiency is 80 % which is remarkably higher than 53 % in 1 mol dm^{-3} KPF_6/EC:PC electrolyte as compared in Fig. S6, and excellent capacity retention is achieved over 350 cycles in Fig. 3 (b). The K//graphite cell shows the initial reversible capacity of ca. 260 mAh g^{-1} with stepwise voltage plateaus attributed to the staging structure, which are similar to those in 0.8 mol dm^{-3} KPF_6/EC:DEC (Fig. S7). Despite, irreversible capacity of 30 mAh g^{-1} is observed in the beginning of an initial potassiation process from 1.2 to 0.7 V. The irreversible capacity might be caused by the competitive reactions between co-intercalation of solvated potassium ions into graphite and electrolyte decomposition forming SEI film on the surface as was reported in the concentrated LiTFSA/dimethyl sulfoxide (DMSO) electrolyte [25]. After the initial cycle, the K/7 mol kg^{-1} KFSA DME/graphite cell demonstrates higher coulombic efficiency and better capacity retention in Fig. 3(c) than those in 0.8 mol dm^{-3} KPF_6/EC:DEC (see detailed data in Fig. S7). Although the highly concentrated electrolyte is viscous, no significant difference in discharge-rate performance of $K_2Mn[Fe(CN)_6]$ is observed between 7 mol kg^{-1} KFSA/DME and 1 mol dm^{-3} KPF_6/EC:PC (Fig. S8 (a)). On the other hand, the graphite electrode in 7 mol kg^{-1} KFSA/DME exhibits better rate performance than that in 0.8 mol dm^{-3} KPF_6/EC:DEC (Fig. S8 (b)). This excellent rate performance of the graphite electrode is consistent with that obtained in the Li cell filled with

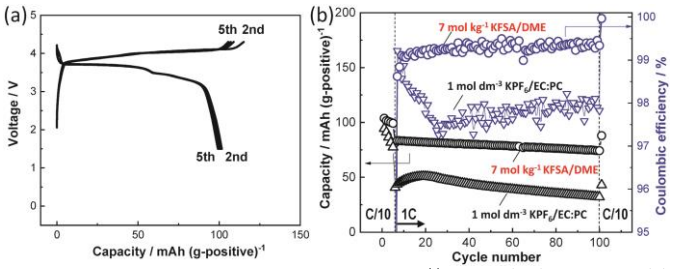

Fig. 4 Electrochemical performance of graphite//$K_2Mn[Fe(CN)_6]$ full-cell: (a) charge/discharge curves of the full cell using 7 mol kg^{-1} KFSA/DME electrolyte with K-metal pretreatment, and (b) cyclability and coulombic efficiency of the full cell using 7 mol kg^{-1} KFSA/DME and 1 mol dm^{-3} KPF_6/EC:PC (1:1 v/v) electrolyte.

a 3.6 mol dm^{-3} LiFSA/DME electrolyte and is possibly attributed to fast de-solvation kinetics or low SEI resistance [16].

Furthermore, a K-ion full cell of graphite/7 mol kg^{-1} KFSA DME/$K_2Mn[Fe(CN)_6]$ was fabricated, and the electrochemical properties were examined. Despite the excellent half-cell performances, the full cell shows an initial reversible capacity of 33 mAh g^{-1} and a large irreversible capacity of ca. 190 mAh g^{-1} (Fig. S9 (a)). The potential curves measured with a three-electrode cell in Fig. S9 (b) reveal that potential plateau at 1.1 V vs. K^+/K for the graphite negative electrode is quite higher than 0.1 – 0.3 V for K intercalation into the graphite, suggesting that the large irreversible capacity originates primarily from the graphite electrode. Though this phenomenon is not understood fully, a possible reason is the decrease in water content in the electrolyte. Actually, the water content in the electrolyte measured by Karl Fisher titration decreased from 43 ppm to 10 ppm by soaking K metal piece into the electrolyte (see Table S2). It is reasonably thought that the lower water content is realized in the K half cells, resulting in the better electrochemical performances. To use the electrolyte containing 10 ppm water in K-ion full cell, K metal was simply soaked in the 7 mol kg^{-1} KFSA/DME solution for two days, then the resultant solution was used as an electrolyte in the graphite/7 mol kg^{-1} KFSA DME/$K_2Mn[Fe(CN)_6]$ full cell. The full cell free from K metal demonstrates reversible charge/discharge behavior in Fig. 4(a) compared with the non-pretreated 7 mol kg^{-1} KFSA/DME electrolyte in Fig. S9 (a). Although some irreversible behavior which possibly leads to lower capacity in the full cell than in half cells is observed in the initial cycle, the full cell delivers a reversible capacity of 104 mAh (g of $K_2Mn[Fe(CN)_6]$)$^{-1}$ with a mean operation voltage of 3.5 V. The full cell achieves excellent capacity retention of more than 85 % after 101 cycles with average coulombic efficiency of 99.3 %, which are much higher than those in 1 mol dm^{-3} KPF_6/EC:PC electrolyte as shown in Figs. 4(b) and S10. Highly concentrated KFSA/DME electrolyte is promising electrolyte for 4 V class KIBs, and further improvements of cycle life and coulombic efficiency are expected by optimizing electrolyte additives.

In summary, KFSA salt shows the highest solubility in carbonate-ester and ether solvents among KFSA, KTFSA, KPF_6, KBF_4, and $KClO_4$, and the KFSA/DME solution shows higher ionic conductivity and lower viscosity in the highly concentrated region compared with those of KFSA/PC and KFSA/GBL. The 7 mol kg^{-1} KFSA/DME electrolyte exhibits a wide potential window of 0 – 4.3 V vs. K^+/K without Al corrosion. Not only the half cells but also the graphite//$K_2Mn[Fe(CN)_6]$ full cell demonstrates higher coulombic efficiency and much better cyclability in the 7 mol kg^{-1} KFSA/DME after pretreatment with K metal than those in a conventional and diluted KPF_6/carbonate ester electrolyte. This promising electrolyte is expected to draw the best performance from electrode materials for high-energy KIBs.

The authors acknowledge Mr. T. Matsuyama for helpful assistance of Karl Fischer titration. This study was partly granted by MEXT program “ESICB”, the JST through A-Step program, and JSPS KAKENHI Grant Number JP16K14103.

Conflicts of interest

There are no conflicts to declare.

Notes and references

1 K. Kubota and S. Komaba, *J. Electrochem. Soc.*, 2015, **162**, A2538-A2550.
2 J. Muldoon, C. B. Bucur and T. Gregory, *Chem. Rev.*, 2014, **114**, 11683-11720.
3 Y. Marcus, *Pure Appl. Chem.*, 1985, **57**, 1129-1132.
4 A. Eftekhari, *J. Power Sources*, 2004, **126**, 221-228.
5 S. Komaba, T. Hasegawa, M. Dahbi and K. Kubota, *Electrochem. Commun.*, 2015, **60**, 172-175.
6 M. Okoshi, Y. Yamada, S. Komaba, A. Yamada and H. Nakai, *J. Electrochem. Soc.*, 2016, **164**, A54-A60.
7 K. Kubota, M. Dahbi, T. Hosaka, S. Kumakura and S. Komaba, *Chem. Rec.*, 2018, **18**, 459-479.
8 M. Morita, T. Shibata, N. Yoshimoto and M. Ishikawa, *Electrochim. Acta*, 2002, **47**, 2787-2793.
9 X. Bie, K. Kubota, T. Hosaka, K. Chihara and S. Komaba, *J. Mater. Chem. A*, 2017, **5**, 4325-4330.
10 C. Zhang, Y. Xu, M. Zhou, L. Liang, H. Dong, M. Wu, Y. Yang and Y. Lei, *Adv. Funct. Mater.*, 2017, **27**, 1604307.
11 J. Liao, Q. Hu, Y. Yu, H. Wang, Z. Tang, Z. Wen and C. Chen, *J. Mater. Chem. A*, 2017, **5**, 19017-19024.
12 Z. Jian, W. Luo and X. Ji, *J. Am. Chem. Soc.*, 2015, **137**, 11566-11569.
13 K. Yoshida, M. Nakamura, Y. Kazue, N. Tachikawa, S. Tsuzuki, S. Seki, K. Dokko and M. Watanabe, *J. Am. Chem. Soc.*, 2011, **133**, 13121-13129.
14 L. Suo, O. Borodin, T. Gao, M. Olguin, J. Ho, X. Fan, C. Luo, C. Wang and K. Xu, *Science*, 2015, **350**, 938-943.
15 K. Matsumoto, K. Inoue, K. Nakahara, R. Yuge, T. Noguchi and K. Utsugi, *J. Power Sources*, 2013, **231**, 234-238.
16 Y. Yamada, M. Yaegashi, T. Abe and A. Yamada, *Chem. Commun.*, 2013, **49**, 11194-11196.
17 K. Takada, Y. Yamada, E. Watanabe, J. Wang, K. Sodeyama, Y. Tateyama, K. Hirata, T. Kawase and A. Yamada, *ACS Appl. Mater. Interfaces*, 2017, **9**, 33802-33809.
18 J. Qian, W. A. Henderson, W. Xu, P. Bhattacharya, M. Engelhard, O. Borodin and J. G. Zhang, *Nat. Commun.*, 2015, **6**, 6362.
19 L. Schafzahl, I. Hanzu, M. Wilkening and S. A. Freunberger, *ChemSusChem*, 2016, **10**, 401-408.
20 J. Lee, Y. Lee, S. M. Lee, J. H. Choi, H. Kim, M. S. Kwon, K. Kang, K. T. Lee and N. S. Choi, *ACS Appl. Mater. Interfaces*, 2017, **9**, 3723-3732.
21 N. Xiao, W. D. McCulloch and Y. Wu, *J. Am. Chem. Soc.*, 2017, **139**, 9475-9478.
22 S. Tsuzuki, K. Hayamizu and S. Seki, *J Phys Chem B*, 2010, **114**, 16329-16336.
23 X. Wang, E. Yasukawa and S. Mori, *Electrochim. Acta*, 2000, **45**, 2677-2684.
24 E. Krämer, S. Passerini and M. Winter, *ECS Electrochem. Lett.*, 2012, **1**, C9-C11.
25 Y. Yamada, K. Usui, C. Chiang, K. Kikuchi, K. Furukawa and A. Yamada, *ACS Appl. Mater. Interfaces*, 2014, **6**, 10892-10899.

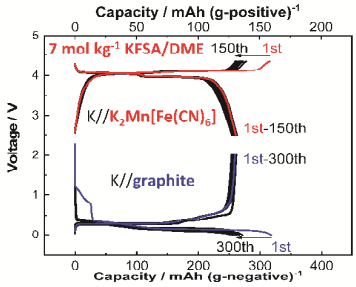

A highly concentrated potassium bis(fluorosulfonyl)amide / 1,2-dimethoxyethane electrolyte solution enables stable cycling of a high voltage potassium-ion battery.